WATER RESEARCH 46 (2012) 3951–3957

Available online at www.sciencedirect.com

SciVerse ScienceDirect

journal homepage: www.elsevier.com/locate/watres

Genetic studies of the role of fatty acid and coenzyme A in photocatalytic inactivation of *Escherichia coli*

Minghui Gao [a], *Taicheng An* [b,**], *Guiying Li* [b], *Xin Nie* [b], *Ho-Yin Yip* [a], *Huijun Zhao* [c], *Po-Keung Wong* [a,*]

[a] *School of Life Sciences, The Chinese University of Hong Kong, Shatin, NT, Hong Kong SAR, China*

[b] *State Key Laboratory of Organic Geochemistry, Guangzhou Institute of Geochemistry, Chinese Academy of Sciences, Guangzhou 510640, China*

[c] *Centre for Clean Environment and Energy, and Griffith School of Environment, Griffith University, Queensland 4222, Australia*

ARTICLE INFO

Article history:
Received 17 November 2011
Received in revised form
12 April 2012
Accepted 17 May 2012
Available online 27 May 2012

Keywords:
Photocatalytic inactivation
Single-gene deletion mutants
Fatty acid composition
Coenzyme A

ABSTRACT

The roles of bacterial cellular components, namely, fatty acid profile and coenzyme A, in photocatalytic inactivation of bacteria were investigated. *Escherichia coli* BW25113, as a "parental strain", and its isogenic single-gene deletion mutants *E. coli* JW1081 (*fabF*$^-$ mutant) and *E. coli* JW3942 (*coaA*$^-$ mutant) showed different susceptibilities towards photocatalytic inactivation by titanium dioxide (TiO_2, irradiated by UVA lamps ($\lambda = 365$ nm)). Regulating the fatty acid composition through pre-incubation temperature adjustment demonstrated the crucial role of cell membrane fatty acid profile in bacterial susceptibility towards photocatalytic inactivation, while the lower coenzyme A level in *coaA*$^-$ mutant correlated well with its lower susceptibility towards photocatalytic inactivation. Furthermore, transmission electron microscopic study demonstrated the photocatalytic destruction process of bacterial cells. This is the first study using single-gene deletion mutants to explore better understanding of the photocatalytic inactivation mechanism of *E. coli*.

1. Introduction

Photocatalytic inactivation, which has been widely recognized from numerous experimental evidences, provides a promising alternative and efficient water disinfection technology of controlling the spread and/or eliminating microbes. However, the photocatalytic inactivation mechanism has not been well established. In particular, the roles of bacterial cellular components as well as the reactive charged and oxidative species in bacterial inactivation are still unknown. Matsunaga et al. (1985) reported the application of TiO_2–UV photocatalysis for the inactivation of three different microorganisms: *Lactobacillus acidophilus*, *Saccharomyces cerevisiae* and *Escherichia coli*. Then, a wealth of information has demonstrated the efficacy of photocatalytic inactivation of various microbes, including bacteria (Sunada et al., 1998; Hu et al., 2006; Benabbou et al., 2007), viruses (Lee et al., 1997; Vohra et al., 2006), and fungi and yeasts (Lonnen et al., 2005; Maneerat and Hayata, 2006).

To ensure the applicability, many studies focused on the photocatalytic inactivation mechanism. The formation of dimers of intracellular coenzyme A (CoA) resulted in the inhibition mechanism of cell respiration and lead to bacterial cell death was first proposed by Matsunaga et al. (1985, 1988), suggesting the photooxidation of CoA is involved in photocatalytic inactivation of bacteria. These findings indicated

* *Corresponding author*. Tel.: +86 852 3943 6383; fax: +86 852 2603 5767.
** *Corresponding author*. Tel.: +86 20 85291501; fax: +86 20 85290706.
E-mail addresses: antc99@gig.ac.cn (T. An), pkwong@cuhk.edu.hk (P.-K. Wong).
0043-1354/$ – see front matter © 2012 Elsevier Ltd. All rights reserved.
doi:10.1016/j.watres.2012.05.033

that TiO_2 photocatalysis induced direct oxidative stress to bacterial components. Saito et al. (1992) demonstrated that photo-activated TiO_2 provoked the rupture of the cell membrane of *Streptococcus sobrinus* using transmission electron microscopy (TEM). Another study reported the photocatalytic degradation of endotoxin, a pyrogenic constituent of the outer membrane of a Gram-negative bacterium, and the result suggests that the cell membrane is the primary target of photocatalytic inactivation (Sunada et al., 1998). Maness et al. (1999) elucidated the photogenerated radicals promoted the peroxidation of the polyunsaturated phospholipid components of the lipid membrane, which lead to respiration loss and cell death. The oxidation of membrane lipids in photocatalytic inactivation was also documented (Huang et al., 2000; Kiwi and Nadtochenko, 2004, 2005; Nadtochenko et al., 2005).

For bacterial inactivation, in general, the cells are attacked by photogenerated reactive charged and oxidative species (ROSs), leading to the damages of cell membrane, cell wall and other intracellular components. Hydroxyl radical (•OH) has been widely accepted as the major ROS responsible for bacterial inactivation (Cho et al., 2004; Khodja et al., 2005; Zhang et al., 2010). Unfortunately, most of these studies investigating the photocatalytic inactivation efficiency based on the study of a single bacterial strain rather than the mechanism, and there is no systematic and comparative study on photocatalytic inactivation of a series of closely related bacterial strains. Also the influences of cellular constituents on photocatalytic inactivation mechanism have not been fully elucidated.

The present study investigates the photocatalytic inactivation of *E. coli* BW25113 (used as a "parental strain") and its two isogenic single-gene knock out mutants – *E. coli* JW1081 (*fabF*$^-$ mutant) and *E. coli* JW3942 (*coaA*$^-$ mutant). Both the parental and its isogenic mutant strains are belonged to the Keio Collection (Baba et al., 2006). In the present study, firstly, photocatalytic inactivation efficiencies of parental and two mutant strains were compared. Then, the relationship between the fatty acid composition at different temperatures, coenzyme A level and the bacterial susceptibility towards photocatalytic inactivation of these bacterial strains were determined and compared. Finally, transmission electron microscopic (TEM) analysis was conducted to reveal the bacterial destruction process in photocatalytic inactivation.

2. Material and methods

2.1. Bacterial strains

E. coli BW25113 ("parental strain"), and its single-gene deletion *fabF*$^-$ mutant (*E. coli* JW1081 carrying the mutation of *fabF759*(*del*)::*kan*, encoding β-ketoacyl-acyl carrier protein (ACP) synthase II) and *coaA*$^-$ mutant (*E. coli* JW3942 carrying the mutation of *coaA755*(*del*)::*kan*, encoding pantothenate kinase) are all derivatives of *E. coli* K-12 (Table 1), and were purchased from the Coli Genetic Stock Center (CGSC, Yale University, New Haven, CT, USA). The bacterial cells were cultured and harvested by the methods described by Leung et al. (2008).

Table 1 – The genetic information of *Escherichia coli* parental strain (*E. coli* BW25113) and its single-gene knock out mutants (*E. coli* JW1081 and *E. coli* JW3942).

Strain name	Deleted gene	CGSC mutation name	Mutation function
E. coli BW25113	None	No	Not appropriable
E. coli JW1081	*fabF*	*fabF759*(*del*)::*kan*	Fatty acid biosynthesis
E. coli JW3942	*coaA*	*coaA755*(*del*)::*kan*	Coenzyme A

2.2. Photocatalytic inactivation

The experimental procedures of photocatalytic inactivation were described in previous reports (Leung et al., 2008; Zhang et al., 2010). In brief, the photocatalytic inactivation was carried out in a photocatalytic inactivation reactor (Fig. S1 in Supplementary Information). The UVA (λ = 365 nm, 15 W, 60 Hz, Cole–Parmer, USA) light intensity was measured by an UVX digital radiometer (UVP, Inc. Upland, CA, USA), and fixed at 0.18 mW/cm^2. The reaction mixture was composed of 100 mg/L TiO_2 (P25, Degussa Corporation, Germany) and 2×10^7 cfu/mL of *E. coli* cells, and the total reaction volume was 50 mL. In the pre-incubation experiment, the harvested cells were pre-incubated at different temperatures (10, 25, 30, 37 and 45 °C) for 2 h before photocatalytic inactivation. Dark control (TiO_2 alone without UVA irradiation), light control (irradiated by UVA lamps alone without addition of photocatalyst) and negative control (without TiO_2 or UVA irradiation) were included. All the above experiments were carried out in triplicates.

2.3. Fatty acid profile

Fatty acid (FA) profiles of the parental and mutant strains were determined by gas chromatography employing an Agilent HP 6890 Series II gas chromatograph (Hewlett Packard, Pal Alto, USA) coupled with an HP 7863 autosampler and a flame ionization detector (FID). The determination was conducted according to the method of Leung et al. (2008).

2.4. Fluorescent measurement of bacterial coenzyme A content

Coenzyme A (CoA) contents in parental and mutant strains were determined by the CoA assay and fluorescent detection kit (Cayman Chemical Company, Ann Arbor, MI, USA). This fluorescence was analyzed with an excitation wavelength at 385 nm and an emission wavelength at 612 nm (TECAN Magellan, Tecan Group Ltd., Seestrasse 103, CH-8708 Männedorf, Switzerland).

2.5. TEM

The bacterial inactivation process was determined by TEM study. The detailed procedure was described by Cheng et al. (2007). In brief, the collected samples were prefixed by glutaraldehyde and post-fixed by osmium tetraoxide (E.M. grade, Electron Microscopy Sciences, Fort Washington, PA, USA), and were dehydrated in a graded series of ethanol

concentrations and embedded in spurr solution (Electron Microscopy Sciences, Fort Washington, PA, USA) for polymerization. Ultra-thin sections of 65 nm were cut on an ultratome (Leica, Reichert Ultracuts, Wien, Austria), and stained with uranyl acetate and lead citrate on copper grids. Finally, sections were examined under a Hitachi H-7650 transmission electron microscope (Tech comp Ltd., Tokyo, Japan) to observe morphological changes of the bacterial cells.

3. Results

3.1. Photocatalytic inactivation

Fig. 1 shows the photocatalytic inactivation of *E. coli* parental and its single-gene knock out *fabF*$^-$ and *coaA*$^-$ mutant strains by TiO_2 suspension under UVA lamps irradiation ($\lambda = 365$ nm). The choice of TiO_2 dose was 100 mg/L, which was based on the optimization experimental results as shown in Fig. S2 in the supporting information. The dark, light and negative controls showed no obvious reduction in the viable bacterial colony counts compared with the treatments. It means the control experiments did not cause toxic effect to bacterial cells. In fact, *E. coli* can adapt to UVA irradiation (Berney et al., 2007), and most of UV inactivation is due to long time UVC irradiation with high light intensity (Sanz et al., 2007). In the present study, the light source is UVA lamps, emitting UVA (λ = 365 nm), the light intensity is 0.18 mW/cm^2, and the irradiation time is 40 min. Under these conditions, light irradiation did not significantly affect the viability of *E. coli* cells. When TiO_2 irradiated by UVA, 2×10^7 cfu/mL of cells of three bacterial strains were completely inactivated within 40 min (Fig. 1). However, the two mutants showed different susceptibilities towards photocatalytic inactivation as compared to the parental strain. In the first 10 min, the populations of all bacterial strains showed a sharp decrease. In next 20 min, the population of *fabF*$^-$ mutant decreased slightly faster than that of the parental strain (Fig. 1a). On the contrary, the population of *coaA*$^-$ mutant was slowly decreasing (Fig. 1b). However, cells of all three bacterial strains were completely inactivated within 40 min.

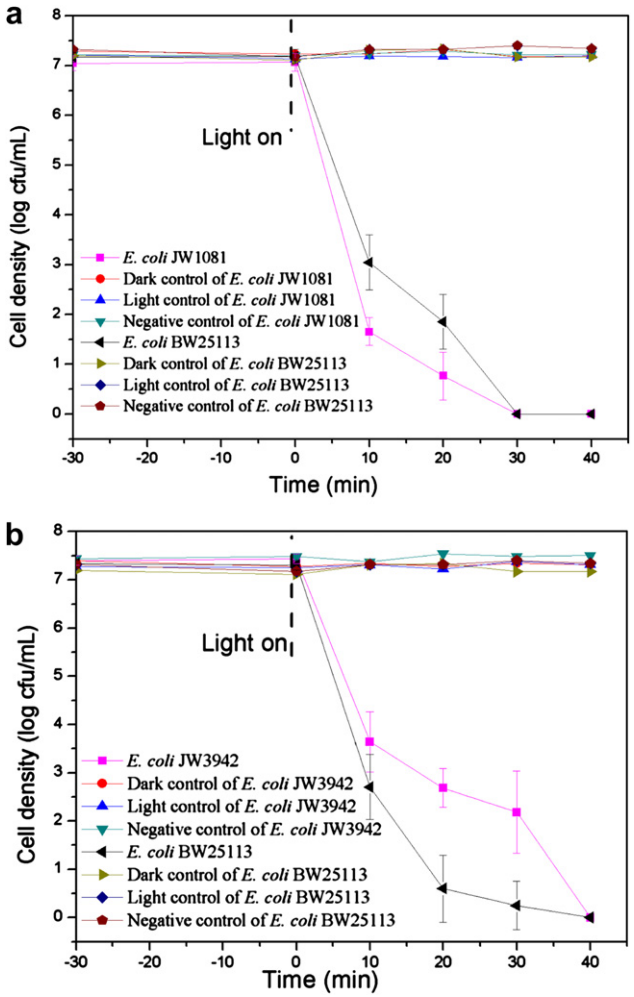

Fig. 1 – Comparison of photocatalytic inactivation efficiencies of (a) parental strain (*E. coli* BW25113) with *fabF*$^-$ mutant (*E. coli* JW1081) and (b) parental strain (*E. coli* BW25113) with *coaA*$^-$ mutant (*E. coli* JW3942). TiO_2 concentration = 100 mg/L, reaction volume = 50 mL, agitation = 200 rpm, temperature = 25 °C, initial cell density = 2×10^7 cfu/mL.

3.2. Effects of pre-incubation at different temperatures

Fig. 2 shows the photocatalytic inactivation of *E. coli* parental and *fabF*$^-$ mutant strains pre-incubated at different temperatures. Control experiments (Fig. S3 in Supplementary Information) in sterile saline solution, at dark and under light irradiation showed that the cells of two bacterial strains did not be inactivated after 2 h pre-incubation at 10, 25, 37, and 45 °C. With the temperature increasing from 10 to 37 °C, the parental strain had a gradual decrease of photocatalytic inactivation efficiency (Fig. 2a). At 10 °C, the photocatalytic inactivation efficiency was the highest for both bacterial strains, while at 37 °C, the cells of the parental strain was the most resistant to photocatalytic inactivation. At 30 °C, the cell of parental strain showed a susceptibility between those at 25 and 37 °C. The photocatalytic inactivation of the parental strain cells pre-incubated at 45 °C was almost the same as that pre-incubated at 30 °C (Fig. 2a). The cells of *fabF*$^-$ mutant pre-incubated at 30–45 °C were also clearly more resistant to photocatalytic inactivation than those pre-incubated at 10 and 25 °C (Fig. 2b). But the cells of *fabF*$^-$ mutant pre-incubated at 30, 37 and 45 °C exhibited the similar resistance towards photocatalytic inactivation (Fig. 2b). Moreover, the populations of parental strain pre-incubated at 30, 37 and 45 °C was reduced to 2.3, 3.3 and 2.2 log, respectively, after 40 min photocatalytic treatment (Fig. 2a); while there were 4.1 log reduction for the populations of *fabF*$^-$ mutant pre-incubated at 30, 37 and 45 °C (Fig. 2b).

3.3. Fatty acid profile

Palmitic acid (16:0) is a representative fatty acid in *E. coli*, but there was only one unsaturated straight chain fatty acid, oleic acid (18:1), detected in the cultures of the parental, *fabF*$^-$ and *coaA*$^-$ mutant strains. Fig. 3 illustrates the ratio of oleic acid (18:1) to palmitic acid (16:0) after the parental and two mutant

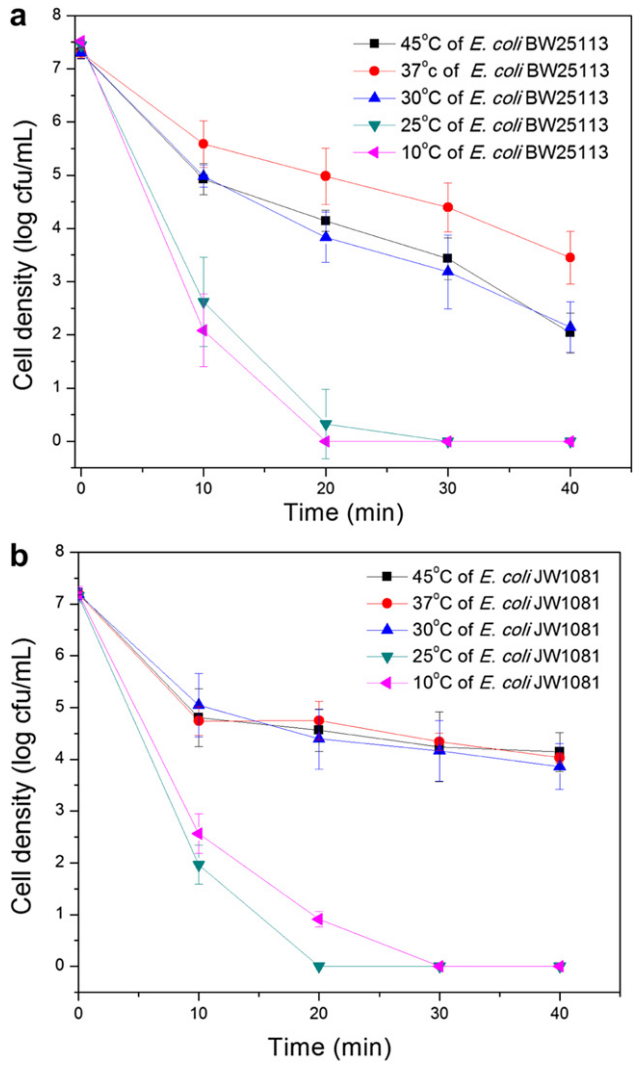

Fig. 2 – Photocatalytic inactivation efficiencies of parental strain (*E. coli* BW25113) and *fabF*$^-$ mutant (*E. coli* JW1081) after 2 h pre-incubation at different temperatures. TiO_2 concentration = 100 mg/L, reaction volume = 50 mL, agitation = 200 rpm, temperature = 25 °C, initial cell density = 2×10^7 cfu/mL. (a) parental strain, and (b) *fabF*$^-$ mutant.

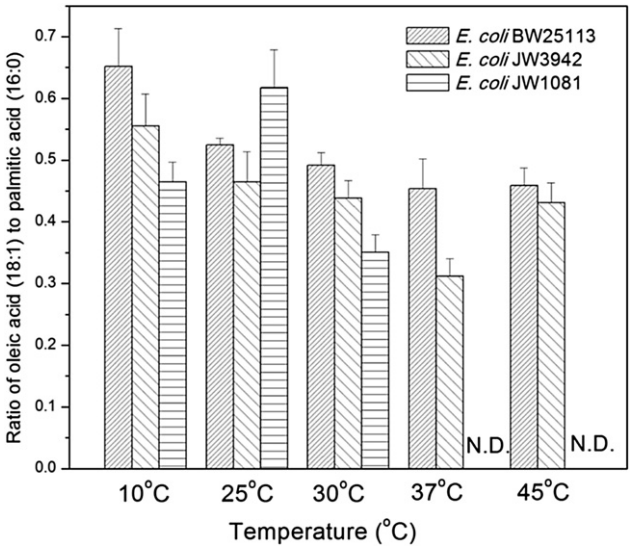

Fig. 3 – Ratio of oleic acid (18:1) to palmitic acid (16:0) after parental strain (*E. coli* BW25113), *coaA*$^-$ mutant (*E. coli* JW3942) and *fabF*$^-$ mutant (*E. coli* JW1081) pre-incubated under different temperatures. N.D. = not detectable.

strains were pre-incubated under different temperatures. With the temperature increase, the ratio of oleic acid (18:1) to palmitic acid (16:0) decreased in the parental and *coaA*$^-$ mutant strains (Fig. 3). However, this decreasing trend was even more obvious for the *fabF*$^-$ mutant. It was noted that at 25 °C, the *fabF*$^-$ mutant possessed a relatively higher ratio of unsaturated to saturated fatty acid than that of the parental and *coaA*$^-$ mutant strains. When temperature increased from 37 to 45 °C, oleic acid (18:1) was not detectable in the *fabF*$^-$ mutant.

3.4. *Fluorescent measurement of bacterial coenzyme A content*

Coenzyme A levels in both parental and mutant strains at their stationary phase were also measured. The cultures of parental and *fabF*$^-$ mutant strains had almost the same level of CoA, and showed a notable higher level than that of *coaA*$^-$ mutant. The CoA level in parental strain is more than one third of that in *coaA*$^-$ mutant (Table 2).

3.5. *Transmission electron microscopy*

Fig. 4 shows the photocatalytic inactivation process at different stages of photocatalytic treatment. Before photocatalytic treatment, the cells exhibited an intact cell structure and an unambiguous cell wall (Fig. 4a). Only after 1 h photocatalytic treatment, the shape of the cell membrane became wavy and partially damaged (Fig. 4b), and after 3 h of irradiation, the cell structure was severely distorted and the center of the cell appeared some translucent region indicating the leakage of the interior components occurred (Fig. 4c). Eventually, with the prolonged photocatalytic treatment, the cytoplasmic contents were completely released outside the cell and the bacterial cell was almost ruptured (Fig. 4d).

4. Discussion

E. coli, a common waterborne bacterium with the best-studied genetics and the largest number of mutant strains, was chosen to investigate the photocatalytic inactivation in this study. The *fabF*$^-$ mutant (*E. coli* JW1081) and *coaA*$^-$ mutant (*E. coli* JW3942) are isogenic single-gene deletion mutants derived from the parental strain (*E. coli* BW25113). The availability of these bacterial mutant strains enables us to determine the role of individual cell structure of *E. coli* BW25113 in photocatalytic inactivation.

The different susceptibilities of different strains towards photocatalytic inactivation (Fig. 1) were probably due to their different genetic properties. The *fabF*$^-$ gene codes for

Table 2 – Coenzyme A levels of parental (*E. coli* BW251113), *fabF*$^-$ mutant (*E. coli* JW1081) and *coaA*$^-$ mutant strains (*E. coli* JW3942).

Bacterial strain	CGSC* mutation	CoA level (mM)
E. coli BW25113	Not appropriable	4.32 ± 0.41
E. coli JW1081	*fabF759(del)::kan*	4.01 ± 0.38
E. coli JW3942	*coaA755(del)::kan*	2.96 ± 0.32

* CGSC = Coli Genetic Stock Center (CGSC, Yale University, New Haven, CT, USA).

a structural gene for β-ketoacyl-ACP synthase II (Rawlings and Cronan, 1992), which is one of the key enzymes involved in fatty acid biosynthesis, particularly in temperature regulating fatty acid composition of *E. coli* (Garwin et al., 1980; Ulrich et al., 1983). Thus the *fabF*$^-$ mutant, carrying a mutation of *fabF759(del)::kan*, cannot produce β-ketoacyl-ACP synthase II. To better understand the role of fatty acid profile in photocatalytic inactivation, the harvested cells of the parental and *fabF*$^-$ mutant strains were pre-incubated at different temperatures before photocatalytic inactivation. The parental strain showed a significant increase of the resistance towards photocatalytic inactivation when it was pre-incubated at increasing high temperatures (Fig. 2a). But *fabF*$^-$ mutant did not show such a gradual increasing resistance (Fig. 2b). At higher temperature (30 and 37 °C), the *fabF*$^-$ mutant became more resistant than the parental strain towards photocatalytic inactivation (Fig. 2). But at very high temperature (45 °C), it may cause the inactivation of other key cellular enzymes, thus both the parental strain and *fabF*$^-$ mutant did not grow well and were comparatively less resistant towards photocatalytic inactivation (Gügi et al., 1991). For the parental strain, at high temperatures (30 and 37 °C), β-ketoacyl-ACP synthase II was less active and thus the synthesis rate of oleic acid (18:1) was decreased. There was no oleic acid (18:1) detected in the *fabF*$^-$ mutant pre-incubated at 37 and 45 °C (Fig. 3), indicating the *fabF*$^-$ mutant lost its ability to regulate fatty acid profile through temperature changes due to the deletion of *fabF*$^-$ gene.

The different susceptibilities of photocatalytic inactivation of the parental and *fabF*$^-$ mutant strains were significantly related with the ratio of unsaturated fatty acid to saturated fatty acid of the bacterial cells. The more resistant the strain towards photocatalytic inactivation, the lower the ratio of unsaturated fatty acid to saturated fatty acid. The results confirm the role of fatty acid composition of cell membrane on photocatalytic inactivation and agree with our previous study (Cheng et al., 2007). The fatty acid composition determines the cell membrane fluidity, which refers to the viscosity of the lipid bilayer of cell membrane. A fundamental biophysical determinant of membrane fluidity is the balance between saturated and unsaturated fatty acids. Cell membrane composed of more saturated fatty acids is more rigid and viscous (Träuble and Overath, 1973). Furthermore, homeoviscous adaptation (Sinensky, 1974) illustrates that the general trend is an increase in unsaturated fatty acids of cell membrane at lower temperatures and a decrease in unsaturated fatty acids at higher temperatures. This adaptation can serve to maintain the reasonable membrane fluidity of bacteria at various temperatures. The parental and *fabF*$^-$ mutant strains became more resistant towards photocatalytic inactivation at increasing pre-incubation temperatures (Fig. 2), which agreed with the fatty acid composition of membrane (Fig. 3), indicating that the cell became more rigid and more difficult to be attacked by the ROSs generated

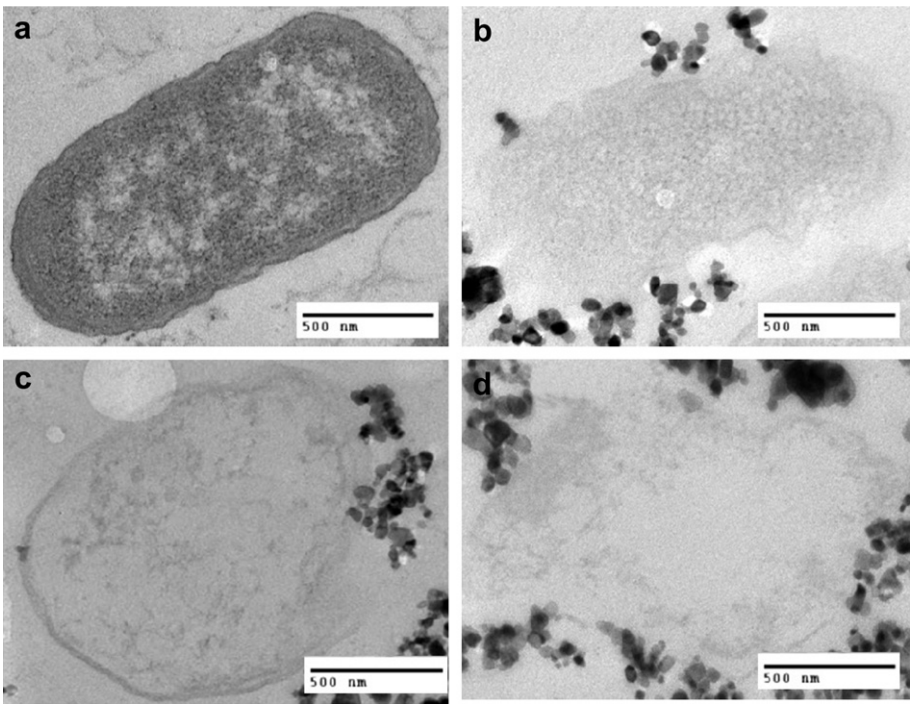

Fig. 4 – TEM images of parental strain (*E. coli* BW25113) untreated or photocatalytically treated with TiO_2 under UVA irradiation. (a) 0 h, (b) 1 h, (c) 3 h and (d) 6 h.

by photocatalysis. The above results suggest that cell membrane is a primary target of photocatalytic inactivation of *E. coli*.

The structural gene *coaA* was located at 90 min of the *E. coli* chromosome, encoding pantothenate kinase synthesis (Song and Jackowski, 1992). Pantothenate kinase as a key regulator of coenzyme A (CoA) catalyzes the rate-controlling step in the CoA biosynthetic pathway (Ivey et al., 2004). The *coaA*$^-$ mutant carries a mutation of *coaA*755(*del*)::*kan*, and has lower CoA concentration than parental strain (Table 2). CoA is known for its role in the fatty acids oxidation. It is an activator of fatty acid oxidation for the first step, acting as the major acyl group (R–CO∼) carrier by reacting with carboxylic acid (R–COOH). Acyl-CoA synthetase of outer mitochondrial membranes catalyzes the activation of fatty acids and esterifies them to CoA, as illustrated in Equation (1).

$$\text{Fatty acid} + \text{ATP} + \text{HS} - \text{CoA} \rightarrow \text{Fatty acyl} - \text{CoA} + \text{PPi\_AMP} \quad (1)$$

With less CoA content, fatty acid activation is probably reduced in *coaA*$^-$ mutant, and may be more difficult to be degraded by ROSs. The lower CoA level in *coaA*$^-$ mutant than that in parental strain correlated well with the greater resistance than parental strain to photocatalytic inactivation (Figs. 1b and 2).

To further understand the destruction process of the cells of the bacterial strains, the structure and morphology of the photocatalytically untreated and treated cells of parental strain were examined by TEM (Fig. 4). With prolonged photocatalytic treatment, eventually, the bacterial cells were completely damaged and lost most of its interior components. The results suggest that the attack by photogenerated ROSs started from the cell membrane of *E. coli*. After damaging the cell membrane and cell wall, the cytoplasmic contents were then released and were photocatalytically degraded.

For photocatalytic inactivation, most studies indicated that bacterial cells are attacked by photogenerated ROSs, such as •OH (Cho et al., 2004; Zhang et al., 2010) and H_2O_2 (Chen et al., 2011; Wang et al., 2011). It has been demonstrated that CoA existing in the cell wall mediated the e^- transfer between bacterial cell and the graphite electrode (Matsunaga and Namba, 1984). Fatty acids were degraded anaerobically (Lalman and Bagley, 2001). Comparing the inactivation efficiencies of parental and *coaA*$^-$ mutant strains, the *coaA*$^-$ mutant is obviously more resistant. It can be interpreted that, with less fatty acid activation, and less CoA mediating e^- transportation, fatty acids probably became difficult to be degraded, and the bactericidal effect is reduced (Fig. 5).

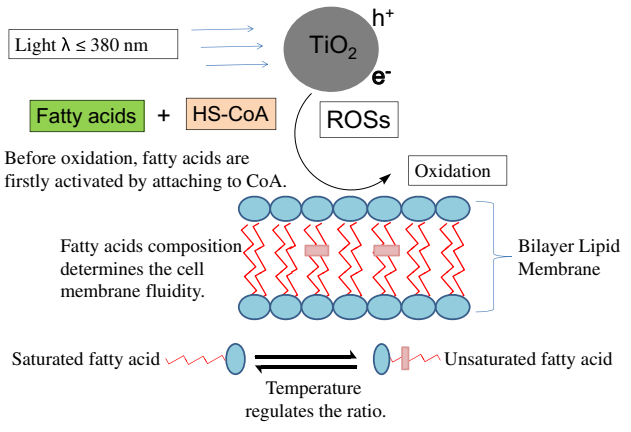

Fig. 5 – The roles of fatty acids, coenzyme A and photogenerated electrons in photocatalytic inactivation.

5. Conclusions

(1) Photocatalytic inactivation was efficient to inactivate the *E. coli* parental and its two isogenic *fabF*$^-$ and *coaA*$^-$ mutant strains. Compared with parental strain, the *fabF*$^-$ mutant was slightly sensitive, while *coaA*$^-$ mutant was less susceptible to photocatalytic inactivation. The different susceptibilities of these bacterial strains are due to their different physiological and genetic properties.

(2) The fatty acid composition of bacterial cells through temperature adjustment significantly influences the photocatalytic inactivation, while CoA, as an activator of fatty acid oxidation and a mediator for e^- transportation, also plays an important role in photocatalytic inactivation.

(3) The results of comparing the susceptibilities towards photocatalytic inactivation of *E coli* parental strain with its two isogenic, precisely defined, single-gene deletion mutant strains, provide a novel genetic approach to investigate the roles of bacterial cellular components in photocatalytic inactivation.

Acknowledgments

The project was supported by a research grant (GRF476811) of the Research Grant Council, Hong Kong SAR Government to P.K. Wong and a research grant (NSFC21077104) of National Science Foundation Council to G.Y. Li and T.C. An. The authors also thank Mr. Freddie Kwok of The Chinese University of Hong Kong for the technical assistance in TEM study.

Appendix A. Supplementary material

Supplementary data related to this article can be found online at doi:10.1016/j.watres.2012.05.033.

REFERENCES

Baba, T., Ara, T., Hasegawa, M., Takai, Y., Okumura, Y., Baba, M., Datsenko, K.A., Tomita, M., Wanner, B.L., Mori, H., 2006. Construction of *Escherichia coli* K-12 in-frame, single-gene knockout mutants: the Keio collection. Molecular Systems Biology 8 (1), 1–11.

Benabbou, A.K., Derriche, Z., Felix, C., Lejeune, P., Guillard, C., 2007. Photocatalytic inactivation of *Escherichia coli*: effect of concentration of TiO_2 and microorganism, nature, and intensity of UV irradiation. Applied Catalysis B: Environmental 76 (3–4), 257–263.

Berney, M., Weilenmann, H.U., Egli, T., 2007. Adaptation to UVA radiation of *E. coli* growing in continuous culture. Journal of Photochemistry and Photobiology B: Biology 86 (2), 149–159.

Chen, Y., Lu, A., Li, Y., Zhang, L., Yip, H.Y., Zhao, H., An, T., Wong, P.K., 2011. Naturally occurring sphalerite as a novel cost-effective photocatalyst for bacterial inactivation under visible light. Environmental Science & Technology 45 (13), 5689–5695.

Cheng, Y.W., Chan, R.C.Y., Wong, P.K., 2007. Inactivation of *Legionella pneumophila* by photocatalytic oxidation. Water Research 41 (4), 842–852.

Cho, M., Chung, H., Choi, W., Yoon, J., 2004. Linear correlation between inactivation of *E. coli* and OH radical concentration in TiO_2 photocatalytic inactivation. Water Research 38 (4), 1069–1077.

Garwin, J.L., Klages, A.L., Cronan Jr., J.E., 1980. *Beta*-ketoacyl-acyl carrier protein synthase II of *Escherichia coli*: evidence for function in the thermal regulation of fatty acid synthesis. The Journal of Biological Chemistry 255 (8), 3263–3265.

Gügi, B., Orange, N., Hellio, F., Burini, J.F., Guillou, C., Leriche, F., Guespin-Michel, J.F., 1991. Effect of growth temperature on several exported enzyme activities in the psychrotrophic bacterium *Pseudomonas fluorescens*. Journal of Bacteriology 173 (12), 3814–3820.

Hu, X., Hu, C., Qu, J.H., 2006. Photocatalytic decomposition of acetaldehyde and *Escherichia coli* using $NiO/SrBi_2O_4$ under visible light irradiation. Applied Catalysis B: Environmental 69 (1–2), 17–23.

Huang, Z., Maness, P., Blake, D.M., Wolfrum, E.J., Smolinski, S.L., 2000. Bactericidal mode of titanium dioxide photocatalysis. Journal of Photochemistry and Photobiology A: Chemistry 130 (2–3), 163–170.

Ivey, R.A., Zhang, Y.M., Virga, K.G., Hevener, K., Lee, R.E., Rock, C.O., Jackowski, S., Park, H.W., 2004. The structure of the pantothenate kinase-ADP-pantothenate ternary complex reveals the relationship between the binding sites for substrate, allosteric regulator, and antimetabolites. The Journal of Biological Chemistry 279 (34), 35622–35629.

Khodja, A.A., Boulkamh, A., Richard, C., 2005. Phototransformation of metobromuron in the presence of TiO_2. Applied Catalysis B: Environmental 59 (3–4), 147–154.

Kiwi, J., Nadtochenko, V., 2004. New Evidence for TiO_2 photocatalysis during bilayer lipid peroxidation. The Journal of Physical Chemistry B 108 (45), 17675–17684.

Kiwi, J., Nadtochenko, V., 2005. Evidence for the mechanism of photocatalytic degradation of the bacterial wall membrane at the TiO_2 interface by ATR-FTIR and laser kinetic spectroscopy. Langmuir 21 (10), 4631–4641.

Lalman, J.A., Bagley, D.M., 2001. Anaerobic degradation and methanogenic inhibitory effects of oleic and stearic acids. Water Research 35 (12), 2975–2983.

Lee, S., Nishida, K., Otaki, M., Ohgaki, S., 1997. Photocatalytic inactivation of phage Q^{β} by immobilized titanium dioxide mediated photocatalyst. Water Science and Technology 35 (11–12), 101–106.

Leung, T.Y., Chan, C.Y., Hu, C., Yu, J.C., Wong, P.K., 2008. Photocatalytic inactivation of marine bacteria using fluorescent light. Water Research 42 (19), 4827–4837.

Lonnen, J., Kilvington, S., Kehoe, S.C., Al-Touati, F., McGuigan, K.G., 2005. Solar and photocatalytic inactivation of protozoan, fungal and bacterial microbes in drinking water. Water Research 39 (5), 877–883.

Maneerat, C., Hayata, Y., 2006. Antifungal activity of TiO_2 photocatalysis against *Penicillium expansum in vitro* and in fruit tests. International Journal of Food Microbiology 107 (2), 99–103.

Maness, P.C., Smolinski, S., Blake, D.M., Huang, Z., Wolfrum, E.J., Jacoby, W.A., 1999. Bactericidal activity of photocatalytic TiO_2 reaction: toward an understanding of its killing mechanism. Applied and Environmental Microbiology 65 (9), 4094–4098.

Matsunaga, T., Namba, Y., 1984. Detection of microbial cells by cyclic voltammetry. Analytical Chemistry 56 (4), 798–801.

Matsunaga, T., Tomoda, R., Nakajima, T., Nakamura, N., Komine, T., 1988. Continuous-sterilization system that uses photosemiconductor powders. Applied and Environmental Microbiology 54 (6), 1330–1333.

Matsunaga, T., Tomoda, R., Nakajima, T., Wake, H., 1985. Photoelectrochemical sterilization of microbial cells by semiconductor powders. FEMS Microbiology Letters 29, 211–214.

Nadtochenko, V.A., Rincon, A.G., Stanca, S.E., Kiwi, J., 2005. Dynamics of *E. coli* membrane cell peroxidation during TiO_2 photocatalysis studied by ATR-FTIR spectroscopy and AFM microscopy. Journal of Photochemistry and Photobiology A: Chemistry 169 (2), 131–137.

Rawlings, M., Cronan Jr., J.E., 1992. The gene encoding *Escherichia coli* acyl carrier protein lies within a cluster of fatty acid biosynthetic genes. The Journal of Biological Chemistry 267 (9), 5751–5754.

Saito, T., Iwase, T., Horie, J., Morioka, T., 1992. Mode of photocatalytic bactericidal action of powdered semiconductor TiO_2 on mutans streptococci. Journal of Photochemistry and Photobiology B: Biology 14 (4), 369–379.

Sanz, E.N., Dávila, I.S., Balao, J.A.A., Alonso, J.M.Q., 2007. Modeling of reactivation after UV disinfection: effect of UV-C dose on subsequent photoreactivation and dark repair. Water Research 41 (14), 3141–3151.

Sinensky, M., 1974. Homeoviscous adaptation-a homeostatic process that regulates the viscosity of membrane lipids in *Escherichia coli*. Proceedings of the National Academy of Sciences of the United States of America 72 (2), 522–525.

Song, W.J., Jackowski, S., 1992. Cloning, sequencing, and expression of the pantothenate kinase (*coaA*) gene of *Escherichia coli*. Journal of Bacteriology 174 (20), 6411–6417.

Sunada, K., Kikuchi, Y., Hashimoto, K., Fujishima, A., 1998. Bactericidal and detoxification effects of TiO_2 thin film photocatalysts. Environmental Science & Technology 32 (5), 726–728.

Träuble, H., Overath, P., 1973. The structure of *Escherichia coli* membranes studied by fluorescence measurements of lipid phase transitions. Biochimica et Biophysica Acta 307 (3), 491–512.

Ulrich, A.K., Mendoza, D., Garwin, J.L., Cronan Jr., J.E., 1983. Genetic and biochemical analyses of *Escherichia coli* mutants altered in the temperature regulation of membrane lipid composition. Journal of Bacteriology 154 (1), 221–230.

Vohra, A., Goswami, D.Y., Deshpande, D.A., Block, S.S., 2006. Enhanced photocatalytic inactivation of indoor air. Applied Catalysis B: Environmental 64 (1–2), 57–65.

Wang, W., Zhang, L., An, T., Li, G., Yip, H.Y., Wong, P.K., 2011. Comparative study of visible-light-driven photocatalytic mechanisms of dye decolorization and bacterial inactivation by B–Ni-codoped TiO_2 microspheres: the role of different reactive species. Applied Catalysis B: Environmental 108–109 (5–6), 108–116.

Zhang, L., Wong, K.H., Yip, H.Y., Hu, C., Yu, J.C., Chan, C.Y., Wong, P.K., 2010. Effective photocatalytic inactivation of *E. coli* K-12 using $AgBr–Ag–Bi_2WO_6$ nanojunction system irradiated by visible light: the role of diffusing hydroxyl radicals. Environmental Science & Technology 44 (4), 1392–1398.